River, Coastal and Estuarine Morphodynamics: RCEM2011

Understanding and managing the morphology of Rhine Delta branches incising into sand-clay deposits

Kees C.J. SLOFF
Deltares (former Delft Hydraulics) and Delft University of Technology
PO Box 177, 2600 MH Delft, the Netherlands

Ary VAN SPIJK
Rijkswaterstaat Zuid Holland
PO Box 556, 3000 AN Rotterdam, the Netherlands

Esther STOUTHAMER
Utrecht University, Faculty of Geosciences
P.O. box 80115, 3508 TC Utrecht, the Netherlands

Arjan SIEBEN
Rijkswaterstaat Center for Water Management
PO Box 17, 8200 AA Lelystad, the Netherlands

ABSTRACT: In the Rhine-Meuse delta in the south-western part of the Netherlands, the morphology of the river branches is highly dependent on the erodibility of the subsoil. Erosion processes that were initiated after closure of the Haringvliet estuary branch by a dam (in 1970), caused a strong incision of several connecting branches. Due to the geological evolution of this area the lithology of the subsoil shows large variations in highly erodible sand and poorly erodible peat and clay layers. In this study is shown how the geological information can be used to create 3D maps of the erodibility of the sub-soil, and how this information can be used to schematize the sub-soil in computational models for morphological simulations.

Local incisement of sand patches between areas with poorly erodible bed causes deep scour holes, hence increasing the risk on river-bank instability (flow slides) and damage to constructions such as groynes, quays, tunnels, and pipelines. Different types of mathematical models, ranging from 1D (SOBEK) to quasi-3D (Delft3D) have been applied to study the future development of the river bed and possible management options. The results of these approaches demonstrate that models require inclusion of a bookkeeping-layer approach for sub-soil schematization, non-uniform sediment fractions (sand-mud), tidal and river-discharge boundary conditions, and capacity-reduction transport modeling.

For risk-reducing river management it has been shown how the development of the river bed can be addressed on a large scale and small scale. For instance, the use of sediment feeding and fixation of bed can be proposed for large-scale management, while monitoring and interventions at initiation of erosion can be proposed as response to small-scale developments that exceed predefined intervention levels.

1 INTRODUCTION

At the mouth of the river Rhine and the river Meuse in the western part of the Netherlands, the rivers bifurcate into several branches before reaching the North Sea, see figure 1. The branches in the middle-

reaches, Spui, Oude Maas, Noord and Dordtsche Kil rivers (see figure 1), have been eroding significantly after the large southern estuary branch, the Haringvliet, was closed by a barrier around 1970. Consequently the tidal volume is now exchanged entirely through the middle reaches, instead of the original estuary mouth. However, due to large spatial variations in the erodibility of the underlying alluvium, the river bed shows alternating stable or aggrading sections and deep erosion pits instead of a continuous degradation. As a matter of fact, the variable erodibility is a dominating factor for the present morphology of the river bed. Locally at deep pits the stability of river banks and adjacent dikes is at stake. To maintain a stable and safe river, the river manager is faced with difficult questions to keep the irregular bed-development within certain limits.

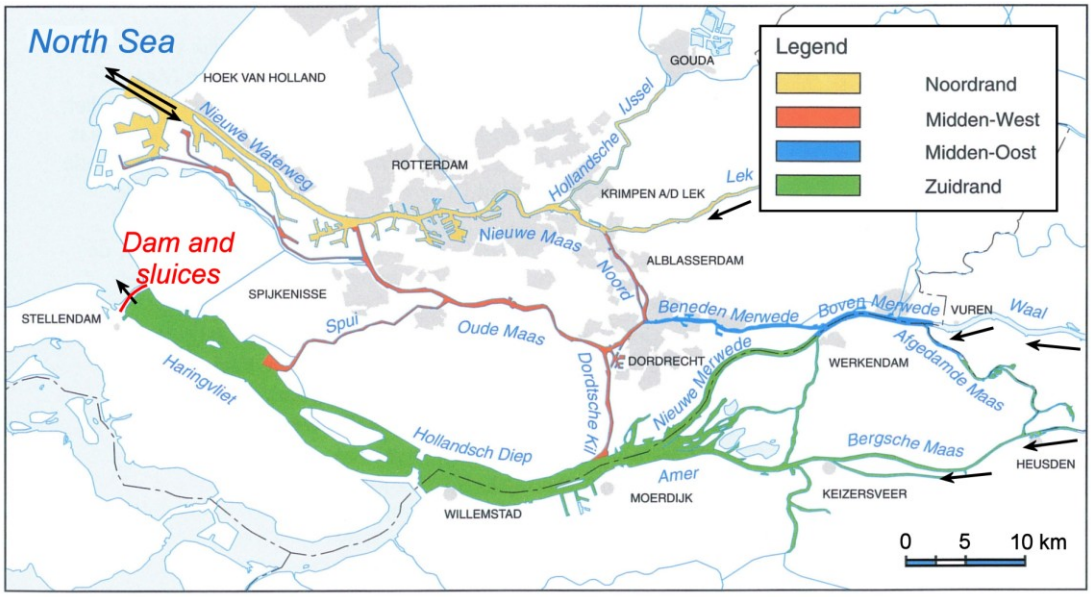

Figure 1 Study area, branches of the Rhine and Meuse River Delta. In this area we distinguish the north-edge (Nieuwe Waterweg and Nieuwe Maas, yellow); the south-edge (Haringvliet and Hollandsch Diep) and the middle-reaches (Spui, Oude Maas, Noord and Dordtsche Kil)

The Holocene Rhine-Meuse delta is formed under the influence of sea-level rise, tectonics, variations in discharge and sediment supply, and storm events. Under the more or less natural conditions that have been prevailing for centuries, this area has been mostly a sediment trap, in which sediment from both the sea and the river were depositing. The varying presence of marshes, avulsions and infilling channels, and so on, has caused the substratum to be composed of alternating layers and patches of sand, clay and peat. An example is shown in figure 2. From paleogeographic reconstruction for the western part of the delta (Hijma, 2009, Hijma and Cohen, 2011) an explanation of the origin of the observed lithostratigraphy has been derived. This reconstruction, as well as the interpretation of a large number of borings and soundings has been used to develop erodibility maps for different levels and characteristic parameters for the stability of side slopes.

As the erodibility of the (compacted) clay layers is much less than that of sand, the large-scale erosion in the middle reaches of the delta does not occur evenly. As indicated above stable (clay) reaches are interrupted by deep scour holes depending on the presence of sand patches in the subsoil. The river managers realize that due the ongoing erosion the risks will increase, and are looking for countermeasures to control the morphological development. We have studied the development of these erosion pits and established a clear relation to the lithology of the fluvial and coastal deposits in which the bed is incising. Next, we have integrated this information into computational models to simulate the morphological development of this system. The use of 1D (SOBEK) and 2D/3D (Delft3D) modeling approaches demonstrates that model require inclusion of a bookkeeping-layer approach for sub-soil schematization, non-uniform sediment fractions (sand-mud), tidal and river-discharge boundary conditions, and capacity-based transport modeling.

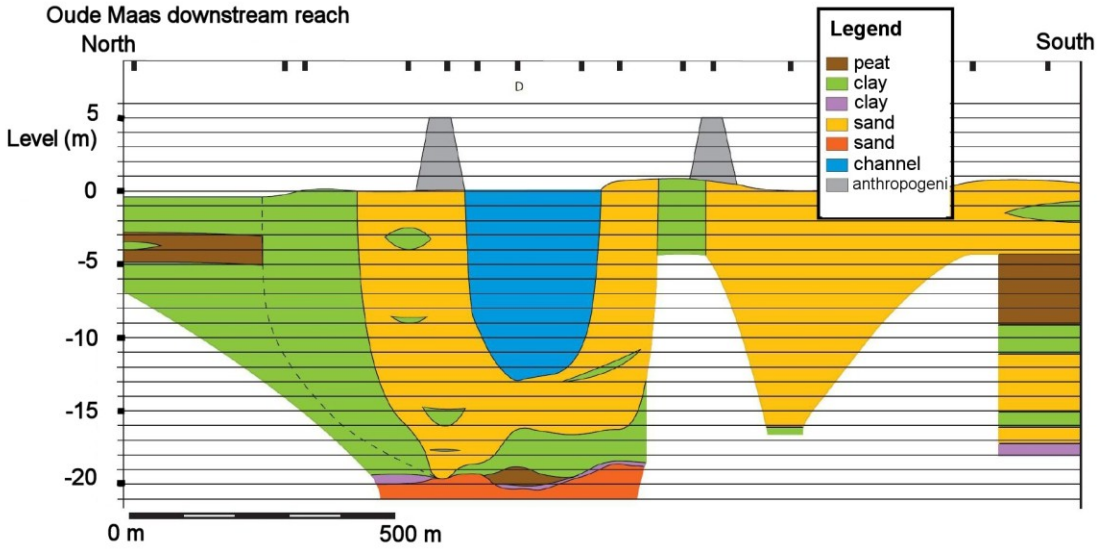

Figure 2 Cross-section from North (left) to South (right) showing the lithology of the substratum of the Oude Maas river branch

For river management it has been shown how the development of the river bed can be addressed on a large scale and small scale. For instance, the use of sediment feeding and fixation of bed can be proposed for large-scale management, while monitoring and interventions at initiation of erosion can be proposed as response to small-scale developments.

2 IMPACT OF NON-HOMOGENEOUS ERODIBILITY OF SUBSTRATUM

If river channels are incising into underlying bed material (substratum) with varying erodibility, the morphology becomes rather distinctive. In figure 3 is sketched how by a breach of poorly erodible (clay) layer the underlying sand gets locally exposed. At this location a large erosion pit develops. The erosion depth of this pit is determined by two conditions:

- Sediment transport on the poorly-erodible bed is under supplied, i.e. the supply of sediment to this reach is less than the transport capacity;
- Local pits attract flow, which strengthens the erosion rate. This phenomenon is discussed by Mosselman and Sloff (2002), who describe situations where large scour holes near structures, attract channels, and hence amplifying the scour holes.

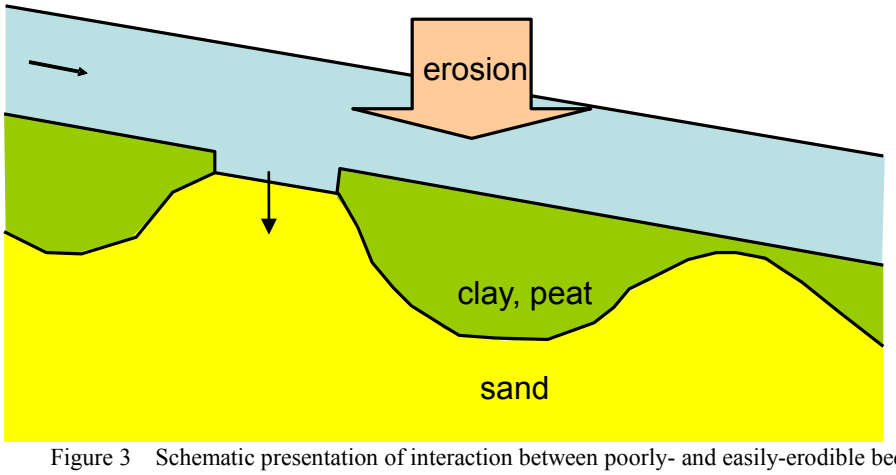

Figure 3 Schematic presentation of interaction between poorly- and easily-erodible bed, and large-scale erosion of the river bed

An example of such a deep erosion pit is shown in figure 4. The erosion depth is about 20 m relative to the bed level in the adjacent river sections, and extending over the full width of the river channel. Because the potential risk of bank instability (flow slides) the dikes in this section have been declared unsafe and stabilizing measures are presently studied. In some other locations the scour holes are extending over only a small part of the cross-section: also in these situations the pits can attain substantial erosion depths.

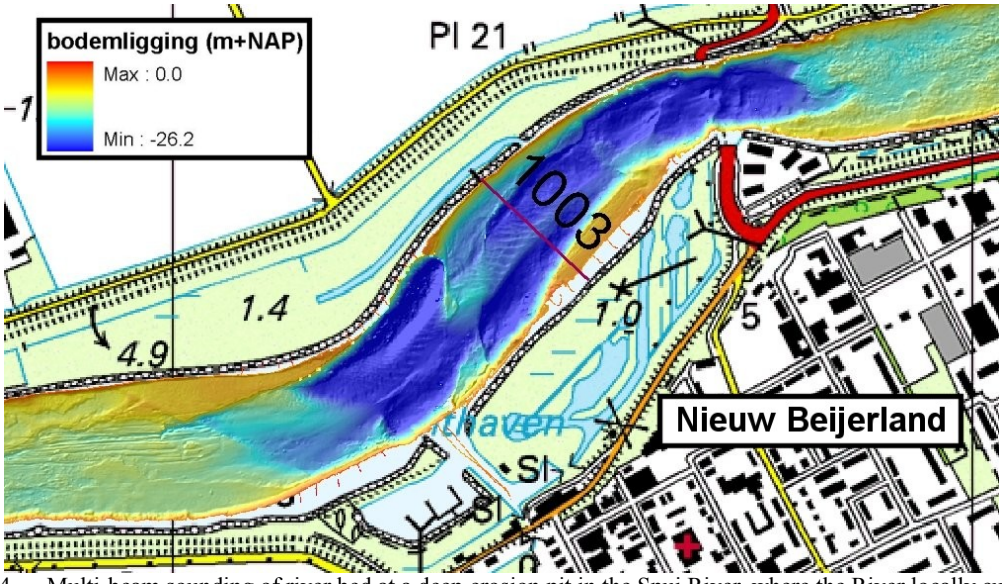

Figure 4 Multi-beam sounding of river bed at a deep erosion pit in the Spui River, where the River locally cuts into a sandy section. Both upstream and downstream of the pit the bed is composed of clay

In upper reaches of the Rhine and Meuse River in the Netherlands an analogous situation occurs where armored gravel layers are formed on top of fine highly-erodible fine sand beds. Due to breaches of the armor layer, rapid erosion will lead to a deep erosion pit. Nevertheless, observations in these reaches show that the erosion may be limited due to a strengthened supply of median-coarse fractions from the adjacent reach (responding to backward erosion), causing a pavement of the bed in the erosion pit. This process does not occur in the lower reaches of the Rhine-Meuse Delta as mobile sediment fractions that can resist the erosive tidal flows (such as coarse gravel) are not available in the bed. Flow velocities by regular tidal flows are in the order of 1 m/s.

3 LITHOSTRATIGRAPHY AND ERODIBILITY OF THE RHINE DELTA BRANCHES

In this study we have constructed the composition of the subsoil under the river bed and of the river banks by synthesis of several available data sources. A very useful data source in this area is the GeoTOP model of TNO (2011), see also Stafleu et al (2008). This model present a 3D database of the Dutch subsoil, containing geological properties (lithology and stratigraphy) of blocks (voxes) with thickness of 0.5 m, on a grid of 100x100 m, up till a depth of 50 m below the surface, see figure 5. The database has been constructed from borings.

We have assigned erodibility to different layers and their characteristics (lithological composition). Therefore we have distinguished between clay, peat and sand, with separation in three classes: low erodibility (hard to erode), moderately erodible, and high erodibility (easy to erode). With this information is was possible to develop erodibility maps for horizontal plains at different depths.

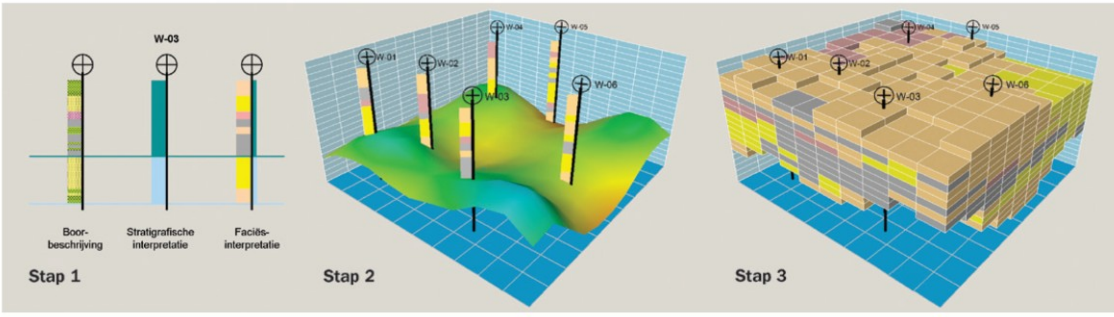

Figure 5 Development and set-up of the GeoTOP model of the subsoil of TNO, interpretation of borings and modeling of stratigraphy and lithoclasses

The erodibility of sand has been determined on basis of the relation between median grain size and the critical Shields value. For the 'Walcheren' and 'Wormer' (Holocene) subsoils the grain size is approximately 175 µm, and the critical Shields value for erosion θ_c = 0.076 (critical shear stress τ_c=0.15 Pa) (Zanke, 2003). For 'Pleistocene' sand we assume a median grain size of 350 µm, and the critical Shields value for erosion θ_c = 0.054 (critical shear stress τ_c=0.30 Pa). The mediane grain size of the sand in the area has been based on the basis of 33 borings by Hijma (2009), as other borings did not have a sufficient description of grain size per layer.

For the erodibility of clay we assume two possible mechanisms:

(1) Consider the mechanism of abrasive erosion. According to Hoffmans & Verheij (1997) the critical shear strength of clay (in [Pa]) can be approached via the critical depth-average velocity u_c:

$$\tau_c \approx 0,7 \cdot \rho_w \cdot \left(r_0 \cdot u_c\right)^2 \qquad (1)$$

in which ρ_w is the density of water [kg/m^3], r_0 is the relative turbulence [-] and u_c is the critical depth-average velocity at which erosion of clay can occur. For moderately soft, consolidated clay u_c = 0.5 m/s. With r_0=0.1 and ρ_w=1000 kg/m^3 this yields τ_c=1.8 Pa. For hard consolidated clay u_c = 1.5 m/s, which yields τ_c=15.8 Pa.

(2) If erosion occurs undrained by pulling-off of fragments of clay or shearing of clay blocks on slopes, undrained shear strength is a measure of critical shear. The undrained shear strength can be related to the cone-resistance and bearing capacity (undrained shear stress = cone resistance/bearing capacity *Nk*). The conce resistance is derived from sounding (cone-penetration tests), while we considered the bearing capacity of holocene clay to be *Nk*=10, and for stiff clay (of the 'Wijchen" layer) *Nk*=20.

For erodibility of peat a correlation function for cone resistance or friction number is not available. Peat erodibility is determined by length, structure and strength of fibers of vegetation in the peat. Considering the analogy in erosion behavior and cone resistance, we assumed that the erodibility of peat also follows from the previously mentioned approach for clay with a bearing capacity *Nk*=10.

In the erodibility map in figure 6 the lithological classes on horizontal sections from the GeoTop model are translated to erodibility classes. Similar to figure 6 we have determined maps for the erodibility classes for each meter depth between 0 to 21 m-NAP. Obviously the sand deposits originating from instance from the former Holocene channel belts are most erodible sections.

Based on the characteristics of the soil from borings and soundings we concluded that the Pleistocene sand is moderately to loosely packed. Sand located above the Pleistocene deposits (Echteld and Wormer formation) is even more loosely packed. Risk on flow slides is relevant for sand layers with loose packing and layer-thickness more than 3 m. In figure 7 is shown, for investigated borings and soundings, at which locations a high risk on flow slides is found. Generally it has been concluded that the risk on flow slides is rather large in the whole area. Especially near the Spui river, where loosely packed sand layers exist between -7 m and the Pleistocene sediment, the risks are high.

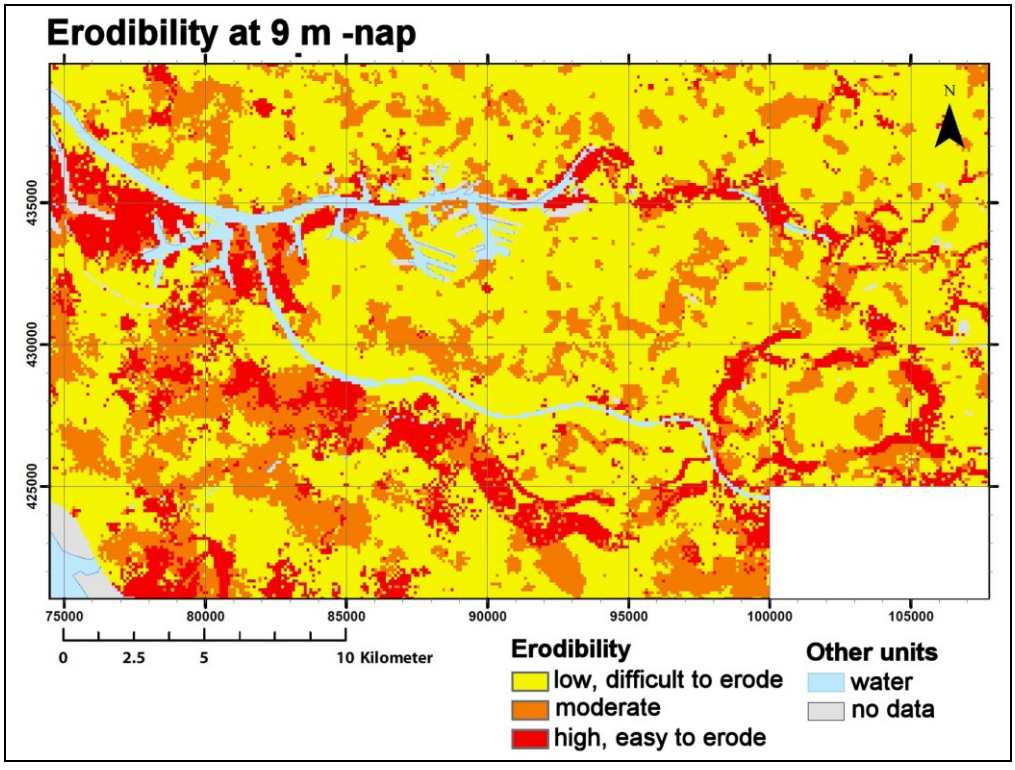

Figure 6 Erodibility map

4 MODELLING APPROACHES

Modeling approaches have been used to analyze the system behavior of the Rhine-Meuse delta, and relate the observed behavior to the interaction between acting processes. Different than other 'conventional' modeling studies, this (eroding) system requires a model that accounts accurately for the interacting erosion processes and subsoil composition.

Initially a one-dimensional calibrated hydrodynamic model for the full delta has been used which is able to simulate the distribution of flows through the various branches accurately. But, it does not simulate morphology and can only be used to estimate the sediment-transport capacity from post processing the flow field using a sediment-transport formula. In this analysis we applied the formula of Engelund and Hansen (1967). In figure 7 is shown how the tidal-average (net) yearly-average sediment-transport capacity for the sand fraction increases along the Spui river branch. The boundary conditions used to get to this result are shown in the right panel in figure 8 (partially). The increase of transport capacity clearly reflects the tendency for erosion. However, as a major part of the bed consists of clay, the potential erosion associated to this transport gradient cannot develop. The results have been used to support analyses on the long-term morphological developments due to sea-level rise, management options, and re-opening the Haringvliet Dam (see also figure 8).

The 1D model can provide a long-term overview of flow distribution in the delta branches as function of river flow and tide. It is possible to extend this 1D model with estuary-equilibrium morphology models (Wang et al., 2007). In this study we have not elaborated this possibility.

To allow a more accurate prognosis of bed-level change and risks of large erosion, we have set-up and used a quasi-3D morphological model for the eastern parts of Delta reach. The aim of this model-approach is to investigate the large-scale morphological response related to the local variability of the bed. The model is an extension of the existing quasi-3D model for the Rhine Branches, as presented by Yossef (2008). We applied the Delft3D modeling system, and set-up a multi-domain model with curvi-linear grids as presented in figure 9. To include the specific details of the varying sediment types in bed and transport we have included a multi-fraction approach with a bed-layer administration. We defined separate size fractions for mud and for sand. The sand fractions are modeled using the transport model of

Van Rijn (2007), while the mud fractions are modeled with the transport model of Krone and Partheniades (1972). Concentrations are calculated with an advection-diffusion approach. Basic equations as applied in the Delft3D modeling system are presented in Lesser et al. (2004).

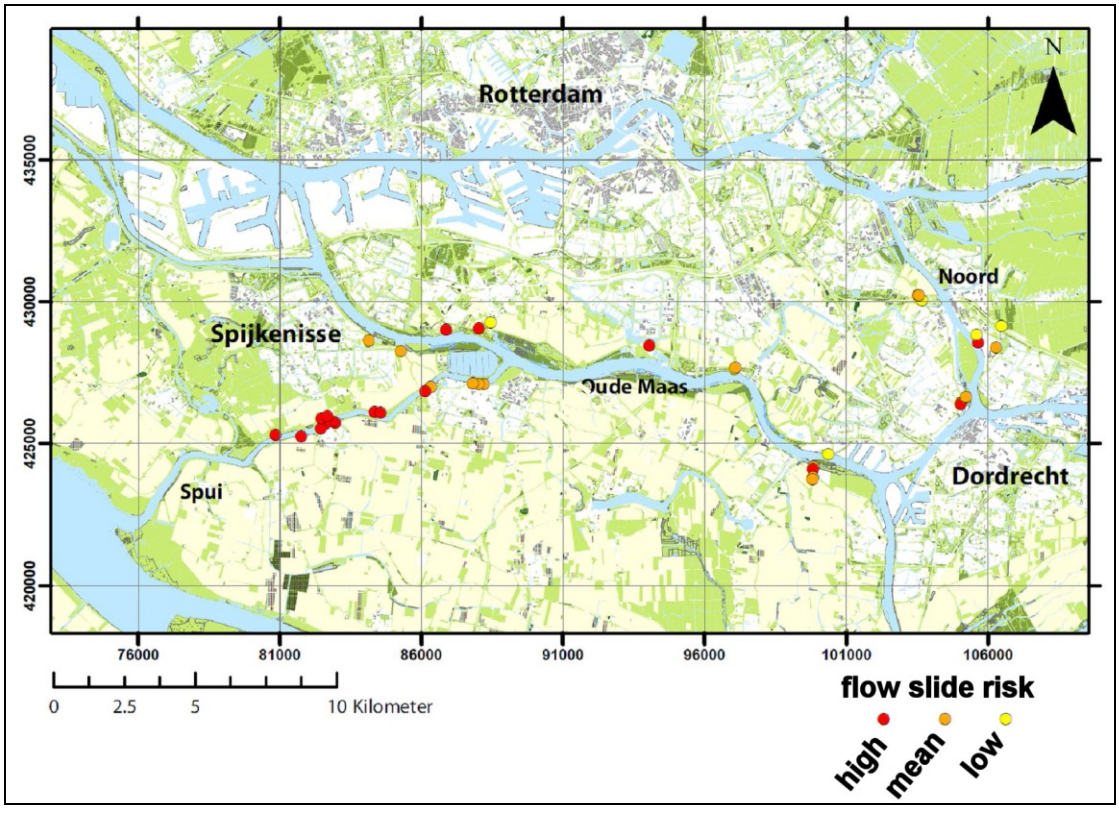

Figure 7 Estimation of flow-slide risk base don borings and sounding in Noord, Oude Maas en Spui rivers

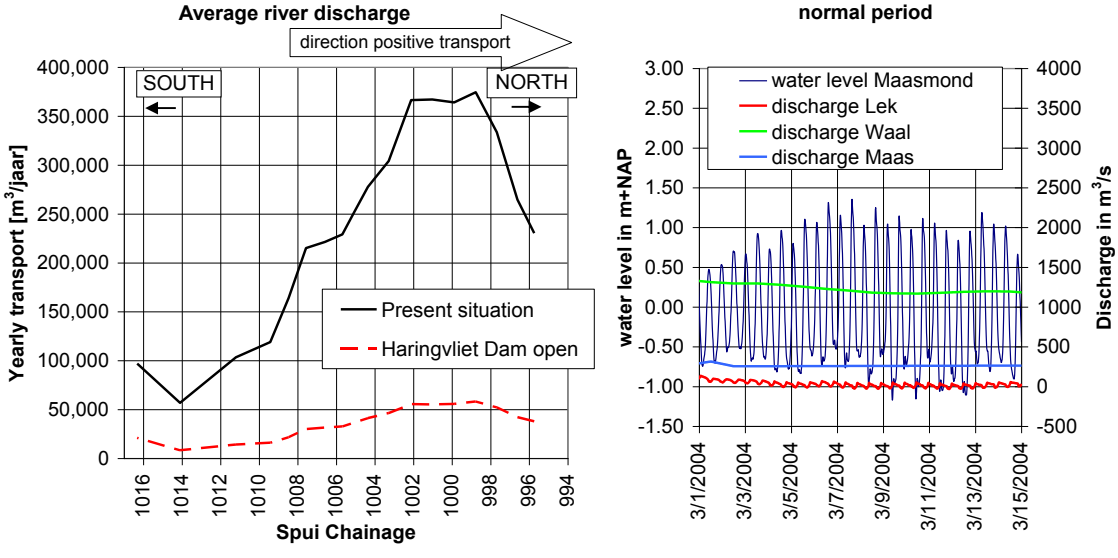

Figure 8 Average net sediment-transport capacity (left) computed with a 1D model for sand. Boundary conditions for 1D model (right)

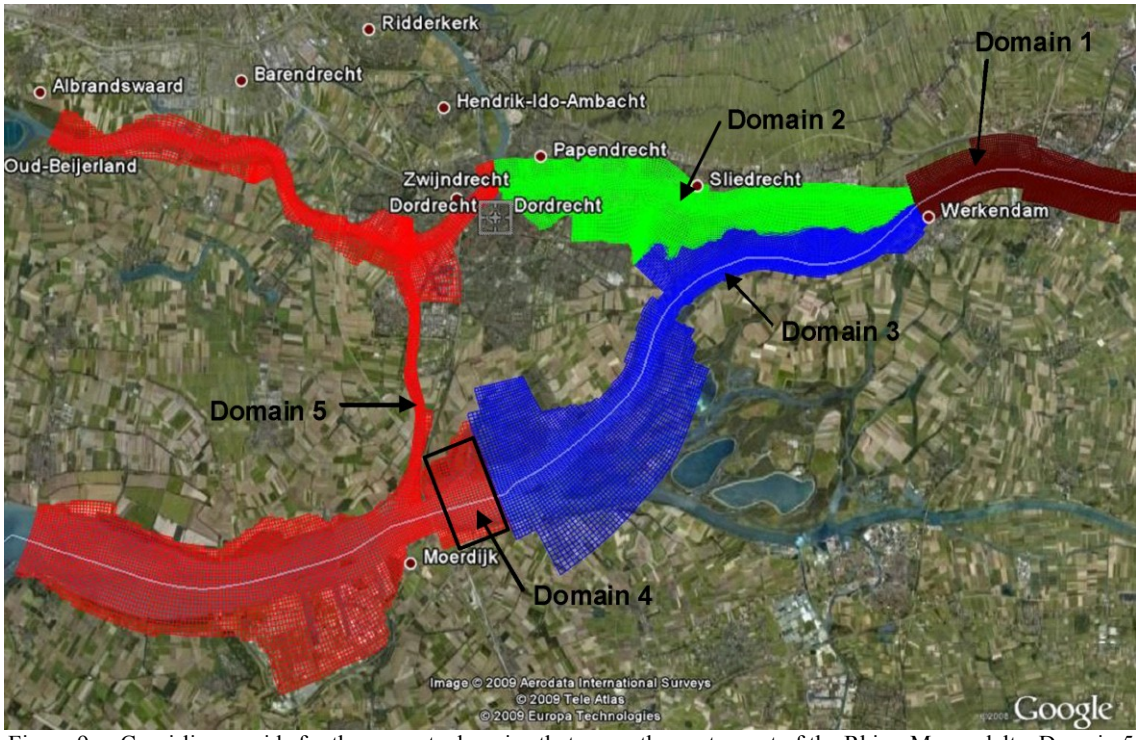

Figure 9 Curvi-linear grids for the separate domains that cover the center part of the Rhine-Meuse delta. Domain 5 is the Dordtsche Kil

The applied transport model of Van Rijn (2007) includes both bed-load and suspended-load transport of non-cohesive (sand) fractions. The suspended-load concentration in this model is used to define source terms in the additional solution of the advection-diffusion of sediment concentration in Delft3D. The formula has been developed as a unified for both wave and currents. However, this study concerns only the 'current' part.

The bed load transport formulation of Van Rijn (2007) reads as follows:

$$q_b = \gamma \rho_s f_{silt} D_{50} D_*^{-0.3} \left(\frac{\tau_b^{'}}{\rho} \right)^{0.5} \left[\left(\frac{\tau_b^{'} - \tau_{b,cr}}{\tau_{b,cr}} \right) \right]^{\eta} \tag{2}$$

with

$$\tau_b^{'} = 0.5 \rho f_c^{'} U_\delta^2 \tag{3}$$

$$f_c^{'} = 8g \left[18 \cdot \log \left(\frac{12h}{k_{s,grain}} \right) \right]^{-2} \tag{4}$$

$$D_* = D_{50} \left[\frac{(s-1)g}{\nu^2} \right]^{1/3} \tag{5}$$

in which, D_{50} = median grain size, D_* = dimensionless particle size; D_{sand} = 62 μm; f_{silt} = silt factor = D_{sand}/D_{50} (f_{silt}= 1 for $D_{50} > D_{sand}$); f_c' = grain friction coefficient due to current; $k_{s,grain}$ = grain-related roughness height; s = relative density of the sediment (~2.65); U_δ = instantaneous current velocity; $\tau_{b,cr}$ = critical shear stress; τ_{b}' = instantaneous grain-related bed-shear stress; γ = calibration coefficient (= 0.5, calibrated value); η = exponent (= 1, calibrated value); ρ = density of water, ν = viscosity of water.

The used Van Rijn formulation incorporates some new features, e.g. the effect of mud fraction on the

critical shear stress of the sand particle that reads as follows:

$$\tau_{b,cr} = \left(1 + p_{mud}\right)^3 \tau_{b,cr,0} \tag{6}$$

in which, $\tau_{b,cr,0}$ = critical bed shear stress for pure sand (Shields curve); p_{mud} = fraction of mud (≤0.3). Note that the mud fraction only affects the mobility of sand in this way, and is not affected by this formula itself.

For computing 2DH suspended sediment transport, a depth-integrated model of Galappatti (Galappatti and Vreugdenhil, 1985) and Wang (1987, 1992) has been implemented in Delft3D, which is based on a first-order analytical solution of the 3D advection-diffusion equation with a concentration or gradient-type near-bed boundary condition. This approach does consider both the non-uniform flow (i.e. spatial variation of concentration in streamwise and transverse directions), as well as the unsteadiness (it is variable with time). The resulting equation can be written as follows:

$$T_A \frac{\partial C}{\partial t} + L_A \frac{\partial C}{\partial x} + L_A \frac{\partial C}{\partial y} = C_e - C \tag{7}$$

where C = depth-average sediment concentration, C_e = depth-average equilibrium concentration; L_A and T_A= adaptation length and time-scales determined by Galappatti's profile functions (derived from expressions for first-order velocity profiles and concentration profiles). In this approach we can define the net sediment entrainment at the bed by:

$$F_s = \left(C_e - C\right) / T_A \tag{8}$$

The reference concentration at level a (i.e., the reference level near the bed) is calculated by using the following expression of Van Rijn (2007):

$$c_a = 0.015\left(1 - p_{clay}\right) f_{silt} \frac{D_{50}}{a} \frac{T^{1.5}}{D_*^{0.3}} \tag{9}$$

Then, the equilibrium suspended sediment load can be calculated as:

$$q_{s,c} = \int_a^h ucdz \tag{10}$$

For mud fractions (cohesive sediment) we apply the modeling formulas of Partheniades-Krone (Partheniades, 1965). In this approach the mud flux from the bed into the water is given by:

$$F_m = E_m - D_m \tag{11}$$

with E_m, D_m being the erosion and deposition rate of mud at the bed respectively. The Partheniades and Krone formulations describe the erosion of mud as:

$$E_m = M\left(\frac{\tau_b}{\tau_{crit,eros}} - 1\right) \mathrm{H}\left[\frac{\tau_b}{\tau_{crit,eros}} - 1\right] \tag{12}$$

$$D_m = -w_s c_{mud}\left(1 - \frac{\tau_b}{\tau_{crit,depos}}\right) \mathrm{H}\left[1 - \frac{\tau_b}{\tau_{crit,depos}}\right] \tag{13}$$

where H[ ] is the Heavi-side function, having a value of 1 if larger than 0, and 0 if less than 0. Furthermore, c_{mud} = concentration of mud, w_s = fall velocity, and M is an empirical erosion parameter.

Critical shear stress for deposition is usually assumed smaller than that for erosion.

In situations with poorly-erodible under layers (e.g., compact clay) under-supplied transport conditions may exist. This means that the amount of sediment available for transport for a certain size fraction (e.g. sand) is less than the local transport capacity. For simulating this type of situations we can consider the under layer fully non-erodible in Delft3D, and remaining undersupplied conditions are simulated using Struiksma's (1999) capacity-reduction approach. Although presently an adapted approach of Tuijnder (2010) is being implemented in the software, which allows simulation of temporary non-erodible layers (clay layers that become erodible at high shear stresses), we have not yet applied this approach to the considered reach.

Using the presented concepts, it is possible to study the combined effect of erodible and non-erodible layers and different sediment types. To illustrate this we show some of the outcomes of the model we have simulated the bed-level development for the Dordtsche Kil branch (the eastern connection between the Haringvliet and the Oude Maas branch). To run the model we impose tidal water-level boundary conditions at the western and northern boundaries, while we impose time-series for discharge at the eastern river boundaries. This is illustrated in figure 10.

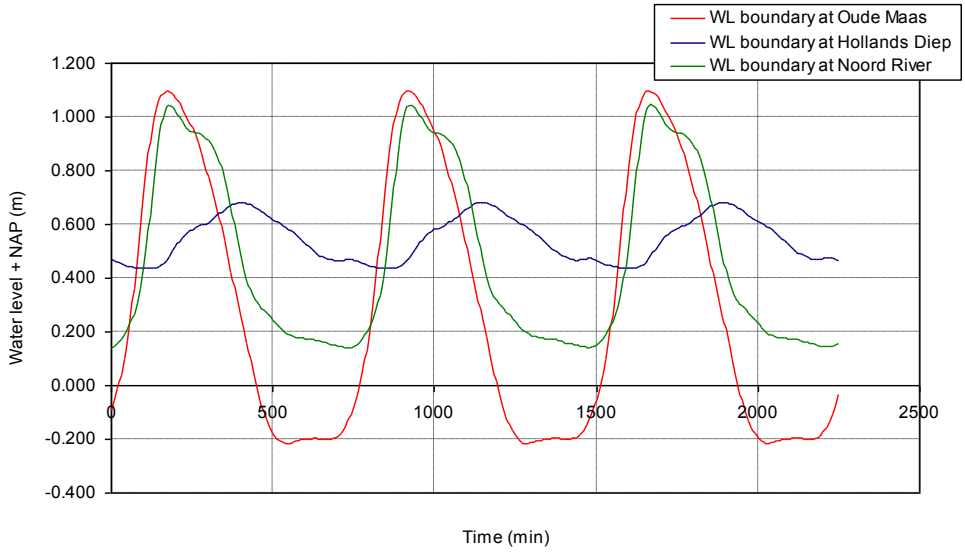

Figure 10 Fragment of a the tidal conditions imposed at the western and northern model boundaries

Note that the relevance of these boundary conditions should not be underestimated. The flow driven by these conditions causes a northward net (tidal-average) sediment transport during low and moderate river flows. However, during high river flows the discharge release-operations at the Haringvliet dam causes the net transport to reverse. Although the high-flow conditions are usually of a limited duration, their impact can be included by running simulation with different discharge regimes.

In figure 11 a sketch is given of the general structure of the subsoil in the Dordtsche kil. The projection of the minimum bed-level in this figure shows that in the northern part the bed is incised in a clay/peat layer. At several locations the river-bed has reached the underlying sand deposits, causing rather deep pits (almost 10 m deeper than adjacent reaches).

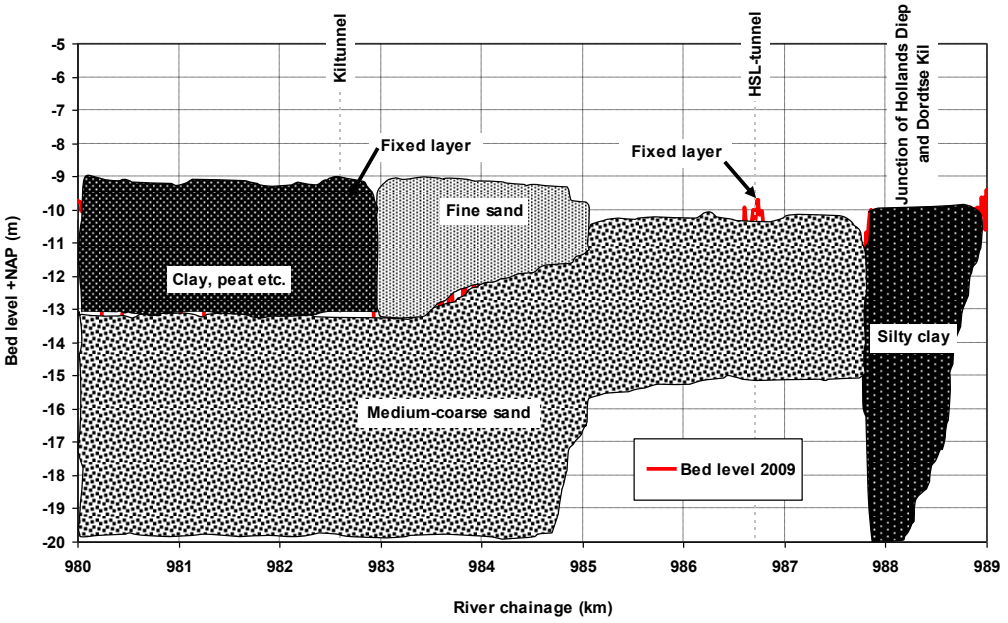

Figure11 An approximate sketch of river bed characteristics along Dordtsche Kil (Bed level is depicted along the river axis, left is North, right is South)

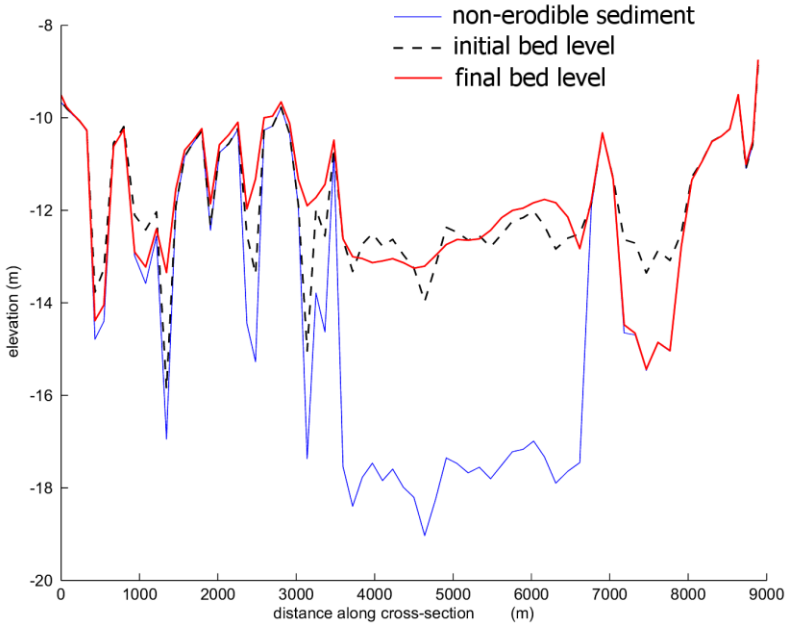

Figure 12 Computed bed-level development along the river axis of the Dordtsche Kil (North is left, South is right); blue line shows the interface between erodible and non-erodible sediment

In Figure 12 the results of a 10-year simulation for Dordtsche Kil has been presented (along the river axis). In this figure is shown how the top of the non-erodible sediment controls the maximum erosion on the southern part of the river (between 7000 - 8000 m). In the northern reaches (between 1000 m - 3500 m) the simulation shows some deposition in the deep pits. This is a temporary infill of sand caused by a passing sediment wave generated by the erosion in the southern and middle reaches (net propagation of sand waves is northward). The bed-level in the axis in the middle reach appears to remain more or less stable. Sediment transport is mostly suspended load.

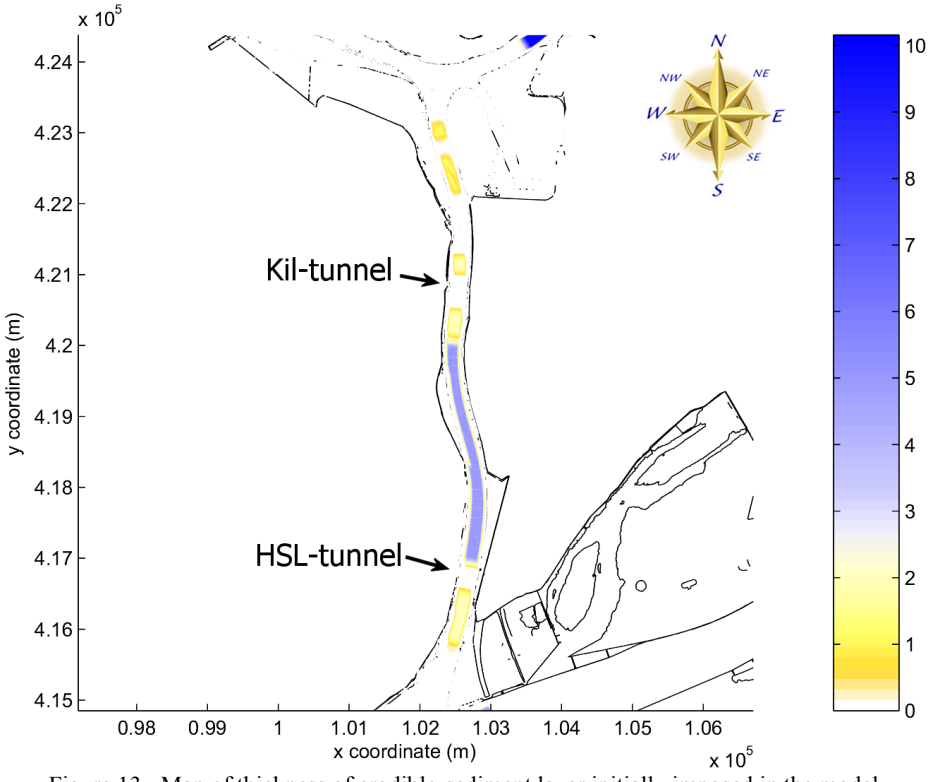

Figure 13 Map of thickness of erodible-sediment layer initially imposed in the model

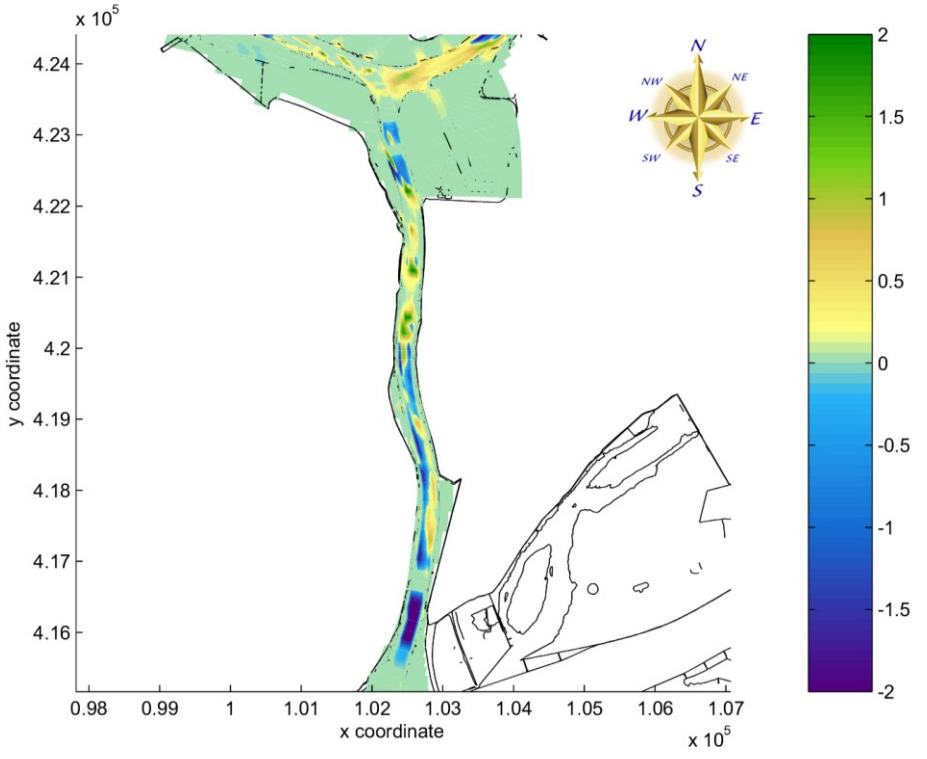

Figure 14 Map of computed bed-level change after 10 year (pos. values are sedimentation, neg. values are erosion)

Some simulation results indicate that the intensity of erosion in the erosion pits is increased in the present undersupplied conditions of the bed and the attraction of flow lines. However, to make a more accurate prediction of growth of these pits more details of 3D scour processes should be added. The lack of these processes in the simulation may also contribute to the strong infilling of the existing erosion pits. Further improvement in this field is foreseen for the future.

In figure 13 the initial layer-thickness of erodible sediment in the computation for the Dordtsche Kil is shown in a map. In this schematization we have defined a constant layer-thickness in transverse direction, roughly based on the observed levels in figure 11. The two tunnels crossing the rivers are completely non-erodible, while we assumed the scour holes in the northern and southern clay layers to be filled with some sand.

The computed bed-level change in figure 14 shows that the observed trends in figure 12 are spatially varying. For instance in the middle reach the western half of the channel eroded, while the eastern half aggraded.

From a comparison of observed bed levels between 2005 and 2009 at Dordtsche Kil, it can be seen that the bed is indeed eroding and that the amplitude of the micro-scale features appear to be decreasing. The erosion appears to be more severe towards the reach just north of the HSL tunnel, and even more pronounced along the east part of the river axis which does not fully correspond to the computed bed-development in figure 14. However, this might also be attributed to the dredging activities in this area that have not been included in the model (dredging activities were carried out during 2007 and 2008, namely ~ 56,000 and 106,000 m^3 respectively). A further improvement of the model results (e.g., including more refined dredging operations) is carried out this year (2011) as part of the applied research project of Deltares.

The outcomes of this study and the tool on itself play an important role in defining sediment management strategies. The model shows time-dependent development of sand deposits, and can be used to support nourishment strategies. Also it shows the gradual erosion of the clay layers, and potential risk of reaching underlying sand layers.

5 MANAGEMENT STRATEGIES

Rijkswaterstaat is the managing organization for the considered river reaches. They are responsible for maintaining the navigability and protecting the surrounding polders against flooding. The protected areas (behind the dikes) are mostly located close to or below sea-level, and prone to inundation. Rijkswaterstaat is therefore preparing a vision on the long-term management of the system. The definition of this vision, aiming on risk reduction, is supported by the knowledge of the acting processes, bed-level development prognoses and composition of bed and banks as presented in this study. The vision is therefore based on the following components:

1. Definition of intervention levels: a minimum and maximum bed level, below and above which intervention is needed. These levels follow from navigation demands (prevent shallows), and from stability criteria of the river banks (prevent deep erosion and steep slopes). Additional criteria, such as protection of tunnels and conduits, as well as controlling salt-intrusion are also relevant for intervention levels.
2. Risks of the present and future bed topography, i.e. does the future development as found from this study invoke further increases of risks.
3. Options for an optimal sediment-management strategy to control the risks, based on the findings of this study.

Minimal intervention levels follow mostly from the criteria for flow slides. An example is given in figure 15, where a slope of maximal 1:7 is prescribed for the slopes in the elevations up to 5 m under the maintenance depth to guarantee stability of the banks. Notably if these banks are composed of loosely packed sand. For river managers these intervention levels can be stored as GIS layers, after which bathymetric measurements can be compared to them, see figure 16. These GIS maps with intervention levels can be defined for all the relevant branches.

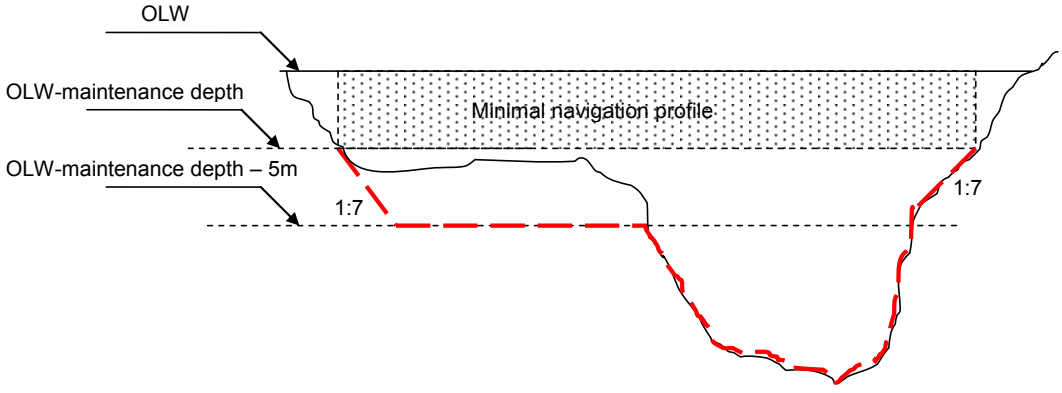

Figure 15 Sketch showing proposed minimal intervention level in a cross-section. OLW is the agreed low water level

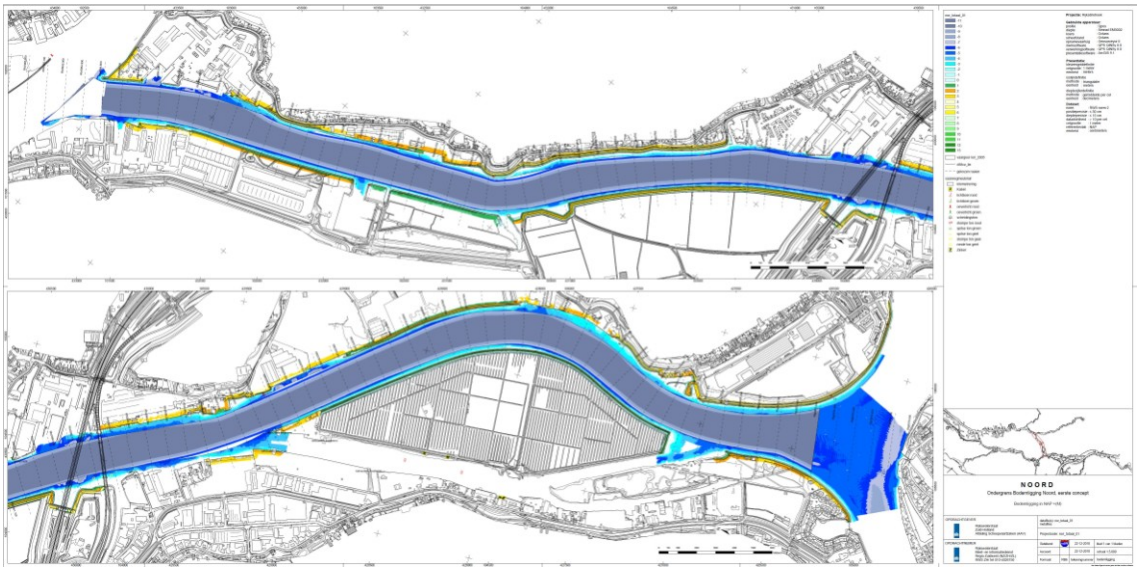

Figure 16 GIS map showing the lower intervention level in the Noord River (dark colors are deepest, light colors are higher)

Considering the system behavior as presented in the previous sections, it has been concluded that for river management the development of the river bed can be addressed on a large scale ad small scale:

- Large-scale developments, such as erosion on the scale of a branch, are slow and can be detected from trends in measured bed topography and model simulations. To manage these developments requires a structural or long-term strategy, and call for preventive measures. For instance, the use of sediment feeding and fixation of bed are proposed. Also the re-opening of the Haringvliet sluices or closure of the connecting branches (Spui and Dordtsche Kil) are possible measures.
- Small scale developments, such as scour holes, are sudden and more difficult to predict. For the response to these developments the intervention levels can be used, provided that an appropriate measurement strategy is set up to allow frequent bathymetric measurements (GIS data). After initiation of the erosion of a scour hole, rapid action is required to stop further erosion for instance by dumping coarse gravel. Allowing the hole to grow means that flow is attracted to it, and protection becomes more and more critical.

Presently (2011) the further elaboration of management strategies is being discussed at Rijkswaterstaat, using the outcomes of this study.

6 CONCLUSIONS

In the Rhine-Meuse delta in the south-western part of the Netherlands, the morphology of the river branches is highly dependent on the erodibility of the subsoil. Erosion processes that were initiated after closure of the Haringvliet estuary branch by a dam (in 1970), caused a strong incision of several connecting branches. In this paper we have presented the outcomes of a study in which a detailed description of the subsoil has been used to define its varying erodibility, and to apply it for analyzing and modeling the river-bed evolution. The aim for this study has been the definition of a vision for managing the river bed in these reaches, based on the understanding of the governing processes.

Simulation with a 1D model show how the existing large-scale gradients in tidal-average (net) sediment-transport rates drive the large-scale erosion trends, and how changes in flow distribution can affect these.

The simulations with a Delft3D model enable prediction of spatially-varying erosion patterns. They revealed that the intensity of erosion in the erosion pits is increased in the present undersupplied conditions of the bed and the attraction of flow lines. However, to make a more accurate prediction of growth of these pits more details of 3D scour processes should be added.

River management options in this study intend to reduce risks of flooding and navigation hindrance. It has been shown how the development of the river bed can be addressed on a large scale and small scale. Large-scale long term bed development is preferably managed by preventive measures, such as the use of sediment feeding and fixation of bed. Small-scale bed development can be managed by responding to exceeding of predefined intervention levels. This requires a monitoring program and interventions at initiation of erosion.

7 ACKNOWLEDGEMENTS

This work was funded by Rijkswaterstaat Zuid Holland and by the applied research program of Deltares. The set-up, execution and analysis of the Delft3D simulations for the Dordtsche Kil were carried out by Dr. Sanjay Giri of Deltares, for which he is greatly acknowledged. Also the contributions of Geeralt van der Ham of Deltares and Vincent Beijk of Rijkswaterstaat Zuid Holland are highly appreciated, and have also played an important role in the end results of this study.

REFERENCES

Engelund, F. & E. Hansen (1967), A monograph on sediment transport in alluvial streams. Teknisk Forlag, Copenhagen.

Galappatti R., and Vreugdenhil C.B. 1985, A depth-integrated model for suspended sediment transport. J. Hydr. Res., IAHR, Vol.23, No.4, p.359-377.

Hijma, M.P. 2009, From river valley to estuary. The early-mid Holocene transgression of the Rhine-Meuse valley, The Netherlands. PhD thesis KNAG/Faculty of Geographical Sciences, Utrecht University, Netherlands Geographical Studies 389, 192p.

Hijma M.P. and Cohen K.M. 2011, Holocene transgression of the Rhine river mouth area, The Netherlands/Southern North Sea: palaeogeography and sequence stratigraphy. Sedimentology. doi: 10.1111/j.1365-3091.2010.01222.x

Hirano M. 1971, River bed degradation with armouring. Trans. of JSCE, Vol. 3, Part 2.

Hoffmans G.J.C.M., and Verheij, H.J. 1997, *Scour manual*. Balkema Rotterdam.

Lesser G. R., Roelvink J.A., van Kester J. A. T. M., and Stelling G. 2004, Development and validation of a three-dimensional morphological model. Jrn. Coastal Engrg., 51,883-915, 2004.

Mosselman, E. and Sloff C.J. 2002, Effect of local scour holes on macro scale river morphology. Proc. River Flow 2002, International Conference on Fluvial Hydraulics, Louvain-la-Neuve, Belgium. Publ. Bousmar, D. & Zech Y. (eds.) A.A. Balkema Publishers, Vol. 2, p. 767-772.

Partheniades, E. 1965. Erosion and deposition of cohesive soils, Journal of the Hydraulic Division, Vol. 91, No.1, S.105 – 139.

Sloff C.J., Mosselman E., and Sieben J. 2006, Effective use of non-erodible layers for improving navigability. In:

Ferreira, R.M.L., E.C.T.L. Alves, J.G.A.B. Leal and A.H. Cardoso (eds.) River Flow 2006, Taylor and Francis/Balkema. Proceedings, p. 1211

Stafleu, J., D. Maljers, J.L. Gunnink, A. Menkovic and F.S. Busschers. 2008, 3D subsurface characterisation of the Netherlands: results from stochastic modelling. In: Mathers, S.J. (ed.). Extended Abstracts of the 2nd International GSI3D Conference, Keyworth, United Kingdom, p. 26

Struiksma, N. 1999, Mathematical modelling of bedload transport over non-erodible layers. Proc. IAHR symposium on River, Coastal and Estuarine Morphodynamics (RCEM), Genova, Sept. 1999, p. 89 – 98.

TNO 2011, website: http://www.dinoloket.nl/nl/about/modellen/geotop.html.

Tuijnder A.P., Ribberink J.S. and Hulscher S.J.M.H. 2009, Morphodynamic modelling of rivers under supply-limited conditions. Proc. IAHR symposium on River, Coastal and Estuarine Morphodynamics (RCEM), Santa Fe, Argentina, Sept. 2009, p. 877 – 882

Van Rijn L.C. 2007, Unified View of Sediment Transport by Currents and Waves. I: Initiation of Motion, Bed Roughness, and Bed-Load Transport; II: Suspended Transport; III: Graded Beds. Journal of Hydraulic Engineering, Vol. 133, No. 6 and 7, June and July, 2007. DOI: 10.1061/(ASCE)0733-9429(2007)133:6(649)

Wang, Z.B. 1989, Mathematical modelling of morphological processes in estuaries. Communications on Hydr. and Geotechn. Engrg., Report No.89-1, Delft Univ. of Techn., Delft, 208 pp (doctoral thesis).

Wang, Z.B. 1992, Theoretical analysis on depth-integrated modelling of suspended-sediment transport. J. Hydr. Res., IAHR, Vol.30, No.3, p.403-421.

Wang Z.B., de Vriend H.J., Stive M.J.F., Townend, I.H. 2007, On the parameter setting of semi-empirical long-term morphological models for estuaries and tidal lagoons. In: Dohmen-Janssen & Hulscher (eds) *RCEM 2007*, published 2008 Taylor & Francis Group, London. P.103-111.

Zanke U. C. E. 2003, On the influence of turbulence on the initiation of sediment motion, Int. J. Sediment Res., 18(1), 1– 15.